CHEMBIOCHEM

ChemPubSoc Europe

DOI: 10.1002/cbic.201200223

Novel Indanone Derivatives as Potential Imaging Probes for β-Amyloid Plaques in the Brain

Jin-Ping Qiao,[a] Chang-Sheng Gan,[b] Chen-Wei Wang,[a] Jin-Fang Ge,[a] Dou-Dou Nan,[a] Jian Pan,[b] and Jiang-Ning Zhou*[a]

Molecular imaging probes to detect senile plaques (SPs) might help the early diagnosis of Alzheimer's disease (AD). In this study, a novel series of indanone derivatives were synthesized and characterized. In in vitro binding studies, compound **2e** exhibited a K_i value of 16 nM with a human AD brain homogenate. Although they displayed relatively low affinities for **2i** and **2j**—with K_i values of 99 and 237 nM, respectively—the SPs in AD brain sections were positively stained by **2j**. A method for in situ micro-autoradiography of AD brain was developed in this study and showed clear labeling of SPs by [^{125}I]**2i** and [^{125}I]**2j**. Both [^{125}I]**2i** and [^{125}I]**2j** had suitable lipophilicities and displayed high initial uptake and rapid clearance from the mouse brains. Furthermore, [^{125}I]**2i** and [^{125}I]**2j** were more stable in human brain homogenates than in mouse brain homogenates. These data suggest that such indanone derivatives might represent potential amyloid imaging agents for the detection of SPs in AD.

Introduction

Alzheimer's disease (AD), the most common form of dementia, currently afflicts more than 35 million people worldwide, and this number is predicted to increase to 106.2 million by 2050.[1,2] Although great progress towards understanding the disease mechanisms has been made in the last three decades, there remains no cure for AD. The medications currently in use, including donepezil, galantamine, rivastigmine, and memantine, are primarily symptomatic treatments.[3] Early intervention might delay the onset or progression of AD. However, early treatment depends on early disease diagnosis.[4] It has been well established that the major neuropathological characteristic of AD is the presence of senile plaques (SPs), which are composed of β-amyloid (Aβ) protein aggregates, and neurofibrillary tangles (NFTs), which are highly phosphorylated tau proteins. Noninvasive detection of SPs with the aid of positron emission tomography (PET) and single-photon-emission computed tomography (SPECT) imaging tracers has been proposed as a useful tool for the early diagnosis of AD.[5,6]

A number of small molecules—such as derivatives of naproxen, thioflavin T (ThT), and Congo Red (CR)—have been developed for imaging of SPs.[7] In the last few years, some of these small molecules have been labeled with ^{11}C, ^{18}F, or ^{123}I, and have been evaluated in PET or SPECT studies in AD patients to test their abilities to detect SPs in vivo (Scheme 1).[8–11] The most widely studied amyloid probe to date—[^{11}C]PIB[12,13]—is limited for routine clinical use by the radioactive decay half-life of ^{11}C (20 min). To overcome the limitation, there are now several amyloid probes labeled with ^{18}F (110 min radioactive decay half-life) under clinical development, such as [^{18}F]BAY94-9172,[14–16] [^{18}F]Florbetapir ([^{18}F]AV-45),[17–19] and [^{18}F]3′-F-PIB.[20–23] Of these, [^{18}F]Florbetapir could become the first ^{18}F-labeled amyloid probe approved by the FDA. These probes still have some limitations, such as white-matter-nonspecific binding higher than that of [^{11}C]PIB.[24,25] [^{123}I]IMPY (**1**),[26–30] the first SPECT probe to be evaluated in humans, displayed a poor signal-to-noise ratio. There is therefore still a need to develop more probes for the imaging of AD brain SPs.

With advances in the study of imaging probes for SPs, the design features of an amyloid probe can be summarized as follows: the molecule should bear at least two phenyl (or heterocyclic) rings and a linker, these two rings should be in conjugation with each other, and the molecule as a whole should be neutral and have a hydrophobic, planarized (or easily planarizable) π system.[31–34]

We searched the database of clinical drugs and found that the scaffold of donepezil matches well with the design features described above. As shown in Scheme 2, it is composed of a heterocyclic ring (indanone group, large dashed-line circle), a phenyl ring (small dashed-line circle), and a linker (piperidine group, large dashed-line box). Because the piperidine group in donepezil, as a flexible structure, is not a proper linker, a double bond (small dashed-line box in indanone derivatives **2**) was introduced as a new linker to generate a conjugated, planarized π system.

[a] J.-P. Qiao, C.-W. Wang, J.-F. Ge, D.-D. Nan, Prof. J.-N. Zhou
CAS Key Laboratory of Brain Function and Disease
School of Life Sciences, University of Science and Technology of China
Room 729, Huangshan Road, Hefei, Anhui, 230027 (P. R. China)
E-mail: jnzhou@ustc.edu.cn

[b] Dr. C.-S. Gan, Prof. J. Pan
Engineering Research Center of Bio-process of Ministry of Education
Hefei University of Technology
Tunxi Road No.193, Hefei, Anhui, 230009 (P. R. China)

Supporting information for this article is available on the WWW under http://dx.doi.org/10.1002/cbic.201200223.

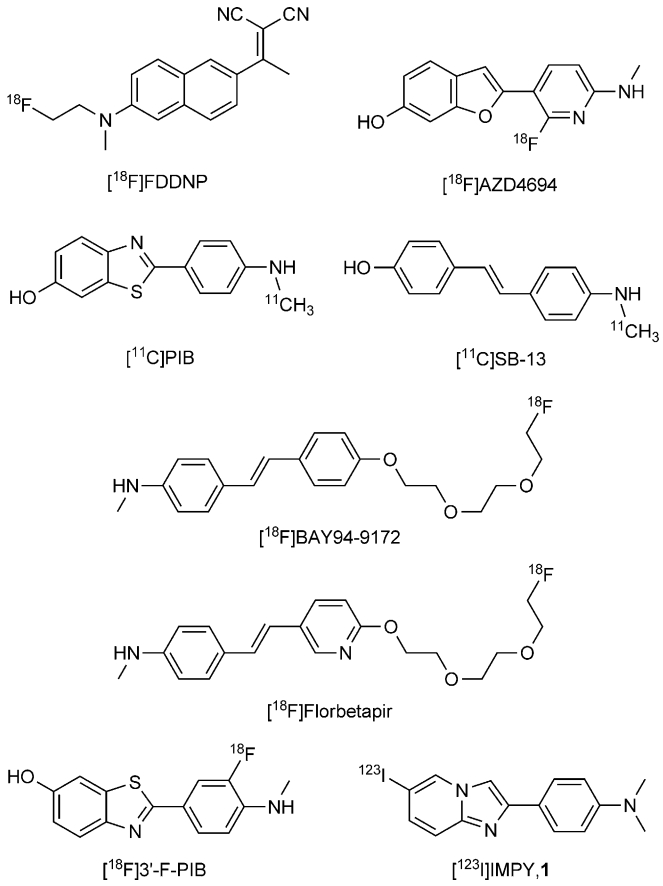

Scheme 1. Chemical structures of clinically evaluated Aβ-plaque imaging probes.

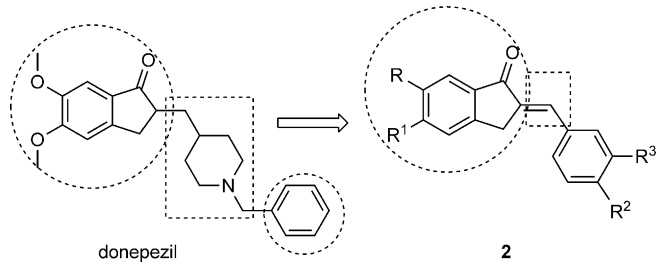

Scheme 2. Design strategy for indanone derivatives.

A series of indanone derivatives were synthesized and their biological activities were assayed. Their potentials as amyloid imaging agents were also evaluated both in vitro and in vivo.[35]

Results and Discussion

Chemistry

The synthesis of target compounds **2a**–**c**, **2e**–**h**, **2j**, and **2k** is illustrated in Scheme 3. The readily available indanones **3a**–**e** and benzaldehydes **4a**–**e** were treated with aqueous NaOH solution (10%) in ethanol at room temperature. Compound **2d** was prepared by heating **2c** in ethanol with the catalyst $SnCl_2{\cdot}2H_2O$. As shown in Scheme 4, 5-hydroxyindan-1-one (**3f**) reacted with 4-(dimethylamino)benzaldehyde (**4d**) in the presence of HOAc and HCl to provide **2l**. The *E* configurations of compounds **2a**–**o** were confirmed by the chemical shifts of the vinyl protons in the ^{1}H NMR spectra. Because of the deshielding effect resulting from the neighboring carbonyl group, the vinyl proton would be expected to give a higher chemical shift in the *E* isomer (>7 ppm) than in the *Z*.[36]

As shown in Scheme 5, 3-bromo-4-(dimethylamino)benzaldehyde (**4f**) was prepared by procedures described previously in the literature.[37] Compound **2m** was prepared from **3a** and **4f** in a procedure similar to that described for compound **2a**. As shown in Scheme 6, compounds **2n** and **2o** were synthesized from **2g** and **2h**, respectively, by treatment with bis(tributyltin) and $Pd(PPh_3)_4$ in Et_3N at 80 °C, and compound **2i** was prepared by treatment of **2n** with iodine in THF at 0 °C.[38]

In vitro binding assay

Radioligand competition binding assays with human AD brain homogenates and use of [^{125}I]**1** as the radioligand were performed to determine the binding affinities of the synthesized compounds.[29] The results are presented in Table 1.

In compounds **2a**–**f**, when the substituents R and R^1 were kept constant as methoxy groups, similarly to the indanone-like system in donepezil, while R^2 was changed, the inhibition constant (K_i) values exhibited large variations. Compound **2e** ($R^2 = NMe_2$) displayed a higher binding affinity ($K_i = 16 \pm 1$ nM) than the others. These results suggest that these compounds likely bind to the SPs through the ThT binding site and likely belong to the class of ThT-type ligands.[7] Next, R^2 was kept constant as NMe_2 while R and R^1 were changed, and the resulting compounds **2e** ($R = R^1 = OMe$) and **2k** ($R = H$, $R^1 = OMe$, $K_i = 21 \pm 1$ nM) displayed increased binding affinities. These results indicate the importance of the NMe_2 and OMe groups in the structures, perhaps because those moieties can form hydrogen bonds (or enter into other interactions) with Aβ aggregates more easily than the others.[7,39–41] Furthermore, from the great affinity contrast between **2m** ($R^3 = Br$, $K_i > 1000$ nM) and **2e** ($R^3 = H$), it can be inferred that the steric bulk or other effect of bromine at the position *ortho* to NMe_2 can lead to unpredictable results. Unlike in the other ThT-type ligands described in the literature,[7] the OMe group at the R^1 (or R) position appears to be important for binding of compound **2** derivatives to Aβ aggregates.

None of the compound **2** derivatives exhibited anti-cholinesterase activity (either acetylcholinesterase (AchE) or butyrylcholinesterase (BChE); see the Supporting Information). This might due to the replacement of the piperidine group by a double bond (Scheme 2).[42] The piperidine group in donepezil had been shown to be important or even essential for anti-cholinesterase activity. These results indicated that as potential SP image probes, compounds **2** might have higher specificities for SPs and fewer side effects (those of anti-cholinesterases, such as diarrhea, nausea, and insomnia).

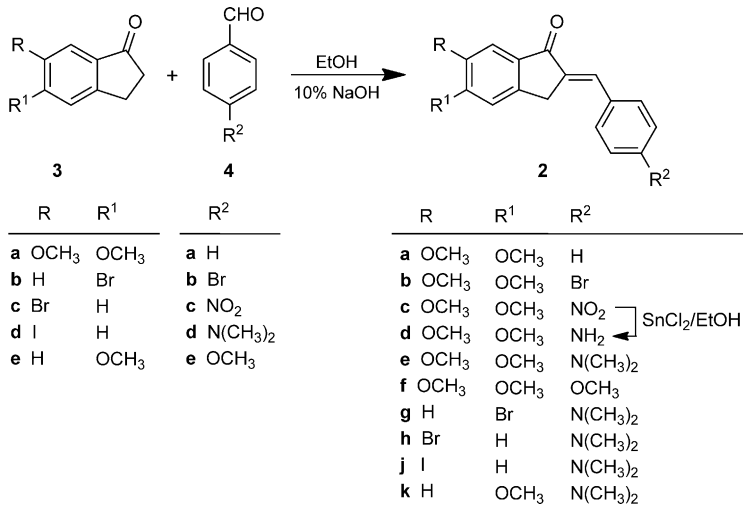

	R	R^1		R^2
a	OCH_3	OCH_3	**a**	H
b	H	Br	**b**	Br
c	Br	H	**c**	NO_2
d	I	H	**d**	$N(CH_3)_2$
e	H	OCH_3	**e**	OCH_3

	R	R^1	R^2
a	OCH_3	OCH_3	H
b	OCH_3	OCH_3	Br
c	OCH_3	OCH_3	NO_2
d	OCH_3	OCH_3	NH_2
e	OCH_3	OCH_3	$N(CH_3)_2$
f	OCH_3	OCH_3	OCH_3
g	H	Br	$N(CH_3)_2$
h	Br	H	$N(CH_3)_2$
j	I	H	$N(CH_3)_2$
k	H	OCH_3	$N(CH_3)_2$

Scheme 3. Synthesis of **2a–h**, **2j**, and **2k**.

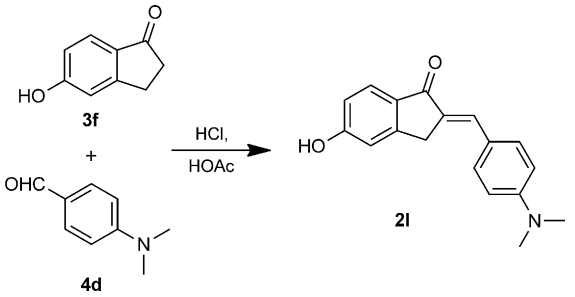

Scheme 4. Synthesis of **2l**.

AD brain tissue fluorescent staining

The scaffold of compound **2** generally shows good fluorescence quantum yields,[43] so fluorescence staining was performed for qualitative visual testing of the abilities of the ligands to bind SPs. As shown in Figure 1, almost all the SPs in the brain section could be labeled by ligand **2j** (C1), as confirmed by staining with CR (A1) and thioflavin S (ThS, B1) in adjacent sections and comparison with the blank control sections (D1). The details of the staining of the SPs were clearly visualized by the fluorescence of **2j** (C2). Interestingly, as shown in Figure 2, the NFTs could also be labeled by **2j** (C4), similarly to the cases of CR (A4) and ThS (B4).

In the fluorescence staining experiments, both **2j** and **2i** were shown to bind to the SPs rapidly (in less than 20 min). It has been postulated that in order to be useful as in vivo SP imaging agents, ligands must have high binding affinities for Aβ aggregates, preferably with K_i values less than 20 nM.[27,44] The K_i values of ligands **2i** and **2j** might therefore not be low enough for them to be viable in vivo agents for Aβ imaging. Nevertheless, the excellent fluorescence staining properties of these two compounds are encouraging. We therefore performed radioiodination and other experiments to characterize these two ligands further.

Radioiodination

The syntheses of the tributyltin precursors (**2n** and **2o**) and the corresponding [^{125}I]-labeled compounds **2i** and **2j** are shown in Scheme 6. Standard iododestannylation reactions with [^{125}I] sodium iodide, hydrogen peroxide, and hydrochloric acid were conducted successfully.[29] Purification of the radiolabeled compounds was performed by HPLC, resulting in 20–30% overall radiochemical yields of the isolated ligands. The chemical identities of the [^{125}I]-labeled ligands were confirmed by co-injection of the labeled compounds with authentic reference standards and coelution of the two compounds on HPLC (Figure 3). The final products—[^{125}I]**2i** and [^{125}I]**2j**—were shown to have radiochemical purities greater than 95% and high specific activities (2200 Ci mmol^{-1}).

Partition coefficient measurement

The partition coefficients (P) of the two radiolabeled ligands [^{125}I]**2i** and [^{125}I]**2j** were measured by conventional octanol/buffer partitioning. For a PET or SPECT tracer, a lipophilicity value, as measured by log P, in the range of 1 to 3 is desirable.[44,45] The log P values of [^{125}I]**2i** (2.80) and [^{125}I]**2j** (2.57) might be predictive of a favorable blood/brain-barrier (BBB) permeability.

Biodistributions in normal mice

To evaluate the brain uptake and biodistribution of the compound **2** derivatives further, in vivo biodistribution studies in normal Institute of Cancer Research (ICR) mice were performed with [^{125}I]**2i** and [^{125}I]**2j** (Table 2). The two radiolabeled ligands each displayed efficient BBB permeability, reaching concentrations of 2.74 and 4.58%, respectively, at 2 min postinjection. The ratios of 60 min to 2 min brain uptake values for these two ligands were 14.5 and 9.8%, respectively, which indicated a fast clearance from normal mouse brains.

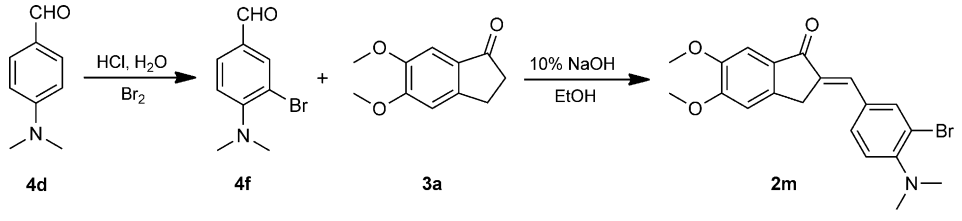

Scheme 5. Synthesis of **2m**.

Stability study

In vitro stability analysis was performed to test the stabilities of the ligands in mouse and human tissues (Figure 4).[46] As shown in Figure 4 (see also Fig-

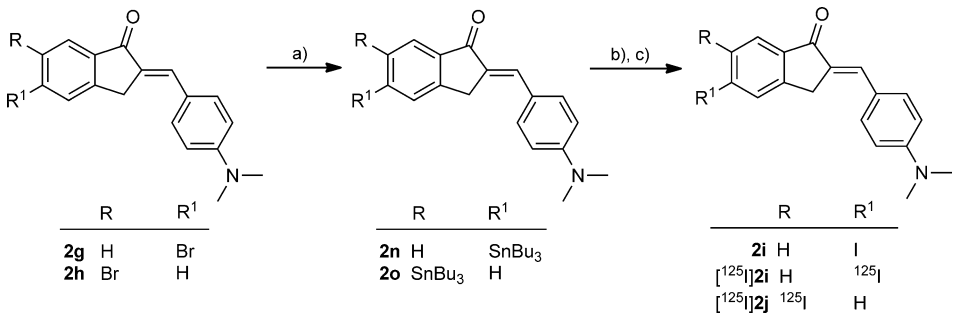

Scheme 6. Synthesis of **2n**, **2o**, **2i**,[^{125}I]**2i**, and [^{125}I]**2j**. a) $Pd(PPh_3)_4$, $(SnBu_3)_2$, Et_3N; b) for **2i**: I_2, THF; c) for [^{125}I]**2i**, [^{125}I]**2j**: Na^{125}I, H_2O_2, HCl, EtOH.

Table 1. Inhibition constants (K_i values) of indanone derivatives upon binding of [^{125}I]**1** to amyloid plaques in AD brain homogenates.

Ligand	R	R^1	R^2	R^3	$K_i \pm$ SEM [nM][a]
2a	OMe	OMe	H	H	>1000
2b	OMe	OMe	Br	H	285±30
2c	OMe	OMe	NO_2	H	>1000
2d	OMe	OMe	NH_2	H	>1000
2e	OMe	OMe	NMe_2	H	16±1
2f	OMe	OMe	OMe	H	111±6
2g	H	Br	NMe_2	H	613±69
2h	Br	H	NMe_2	H	70±2
2i	H	I	NMe_2	H	99±5
2j	I	H	NMe_2	H	237±105
2k	H	OMe	NMe_2	H	21±1
2l	H	OH	NMe_2	H	>1000
2m	OMe	OMe	NMe_2	Br	>1000
1					5±1 (5.0±0.4)[b]

[a] Each value was determined in three separate experiments with duplicate measurements each time. [b] According to the literature.[30]

ure S1 in the Supporting Information), levels of [^{125}I]**2i** were 65 and 13% unchanged after 30 min of incubation in mouse whole blood and mouse brain homogenate, respectively. In contrast, [^{125}I]**2i** was 98 and 98% unchanged after 60 min and 87 and 90% unchanged after 120 min in human AD and control brain homogenates, respectively. Similarly, 46 and 32% of [^{125}I]**2j** remained unchanged after 30 min in mouse whole blood and brain homogenate, respectively. In human AD and control brain homogenates, 98 and 98% of [^{125}I]**2j** was unchanged after 60 min and 90 and 88% of [^{125}I]**2j** was unchanged after 120 min, respectively. The protein contents of the mouse brain (7.02 μg μL^{-1}), human AD brain (12.51 μg μL^{-1}), and control brain (10.79 μg μL^{-1}) homogenates were similar, suggesting that [^{125}I]**2i** and [^{125}I]**2j** might be more stable in the human brain than in the mouse brain.

In vitro autoradiography and in situ micro-autoradiography

Autoradiography (ARG) experiments were performed to test the abilities of the radiolabeled ligands to bind SPs in human brain tissues in vitro. As shown in Figure 5, [^{125}I]**2i** (A2 and B2) and [^{125}I]**2j** (A3 and B3) labeled the SPs in the AD brain sections in similar manner to [^{125}I]**1** (A1 and B1). High concentrations (2 μM) of cold **2i** or **2j** could inhibit no less than 70% of the binding signals of [^{125}I]**2i** and [^{125}I]**2j**, respectively (data not shown). In addition, only a few plaques were labeled in the control sections (C1–C3, D1–D3). These ARG data suggested high signal-to-noise ratios and low nonspecific binding of [^{125}I]**2i** and [^{125}I]**2j**.

To confirm the SP labeling details further, in situ micro-ARG was performed with use of double labeling (radiolabeling and ThS fluorescence staining) to localize SPs. To the best of our knowledge, this was the first use of in situ micro-autoradiography to show single SPs in an amyloid imaging study. As shown in Figure 6, the accurate colocalization of ThS fluorescence and

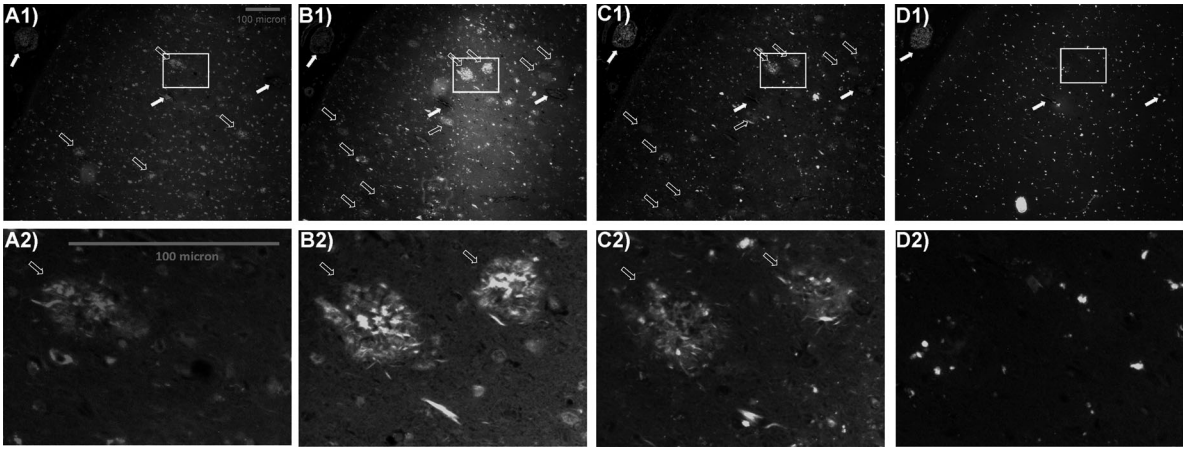

Figure 1. Four adjacent AD brain sections (91-year-old female, Braak 5, temporal cortex, 6 μm thickness) were stained. A) CR. B) ThS. C) **2j**. D) Blank control. The three solid arrows indicate the landmarks. The hollow arrows indicate the amyloid plaques. The images in the bottom row are magnified images of the boxed area in the top row. Scale bars = 100 μm.

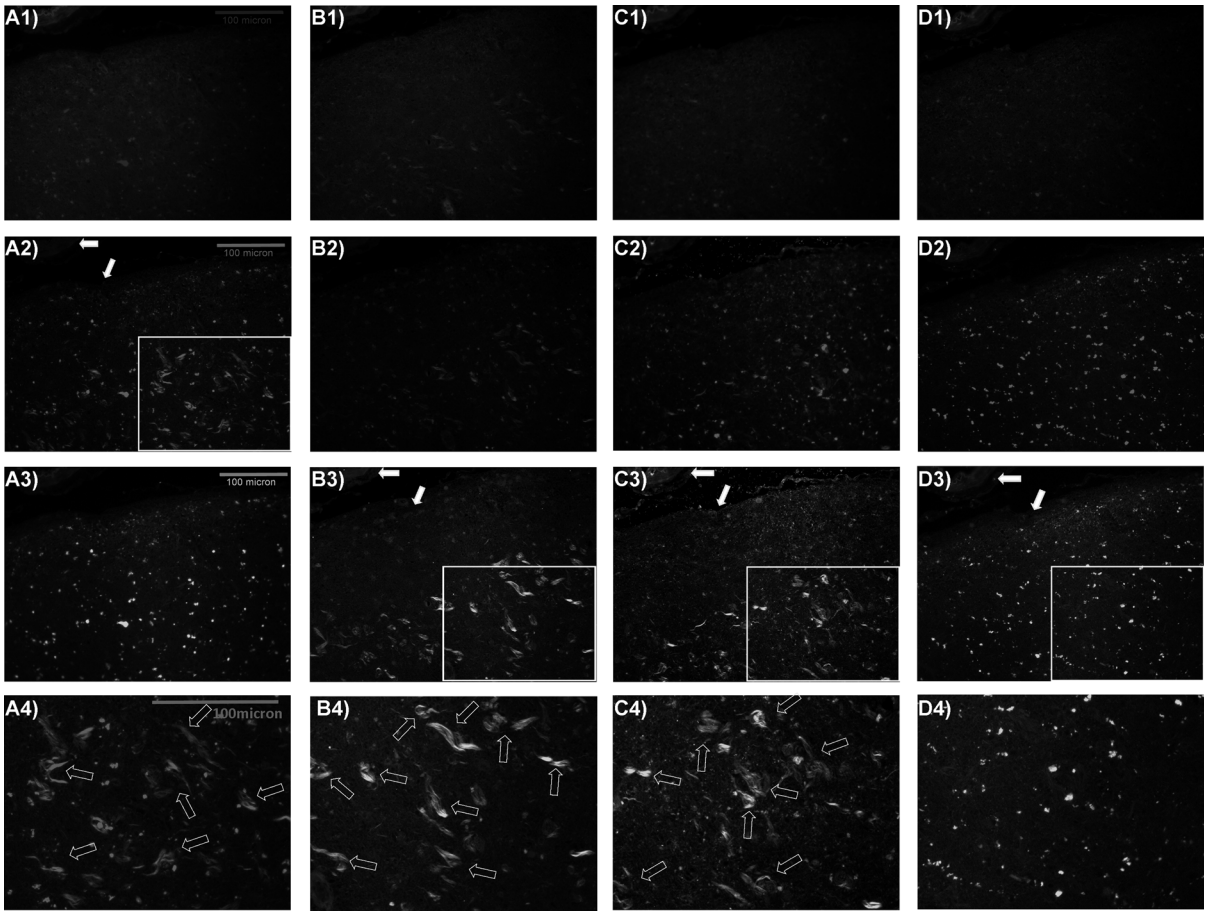

Figure 2. Four adjacent AD brain sections (91-year old female, Braak 5, temporal cortex, 6 μm thickness) were stained. A) CR. B) ThS. C) **2j**. D) Blank control. The two solid arrows indicate the landmarks. The hollow arrows indicate NFTs. The top three rows are the three channels (DAPI, CY3, GFP) of one section. Images A4, B4, C4, and D4 are the magnified images of the boxed area in A2, B3, C3, and D3, respectively. Scale bars = 100 μm.

silver particles (C1–C3) indicated that the ARG signals from the labeled ligands represent SPs.

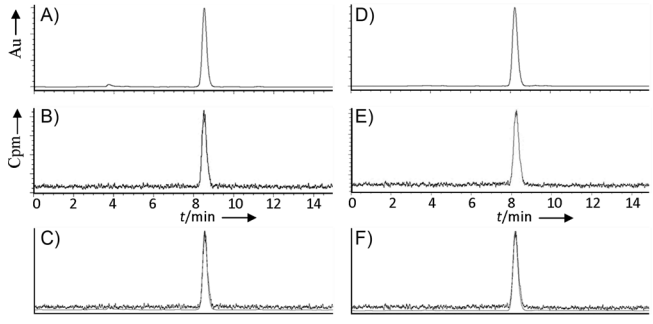

Figure 3. HPLC chromatograms of A) compound **2i**, and D) compound **2j** (blue traces), and of B) radioligand [^{125}I]**2i**, and E) radioligand [^{125}I]**2j** (black traces). Merged UV and γ peaks of C) **2i** and F) **2j**. HPLC parameters: Waters Symmetry C18 analytical column (4.6×250 mm, 5 μm); mobile phase: MeOH/H_2O 9:1; flow rate = 1.0 mL min^{-1}; UV detector at 260 nm. Retention times: t_R = 8.4 min for **2i** (UV), t_R = 8.5 min for [^{125}I]**2i** (γ), t_R = 8.2 min for **2j** (UV), t_R = 8.3 min for [^{125}I]**2j** (γ). The slight retention time differences between the radioactive γ peaks and the UV peaks are due to the configurations of the UV and radioactivity detectors.

The K_i values of **2i** and **2j**—99 and 237 nM, respectively—showed relatively low affinities for binding to the SPs. However, the ARG result seemed to suggest that high binding affinities appear to not be necessary for [^{125}I]**2i** and [^{125}I]**2j** to label SPs, due to the high densities of the SPs in the human AD brain.[44]

Conclusions

In conclusion, we have successfully designed and synthesized a new series of indanone derivatives as potential probes for the in vivo imaging of AD brain amyloid plaques. Of these, compound **2j** clearly stained SPs, and the radiolabeled compounds [^{125}I]**2i** and [^{125}I]**2j** labeled the SPs with intense signals comparable to those provided by [^{125}I]**1**. In biodistribution studies in normal ICR mice, [^{125}I]**2i** and [^{125}I]**2j** displayed good brain penetration and rapid washout from the brain—highly desirable characteristics for in vivo amyloid imaging agents. An in vitro stability study showed that [^{125}I]**2i** and [^{125}I]**2j** were more stable in brain homogenates from humans than in those from mice. Whereas the binding affinities and lipophilicities of the indanone derivatives were comparable to those of IMPY,

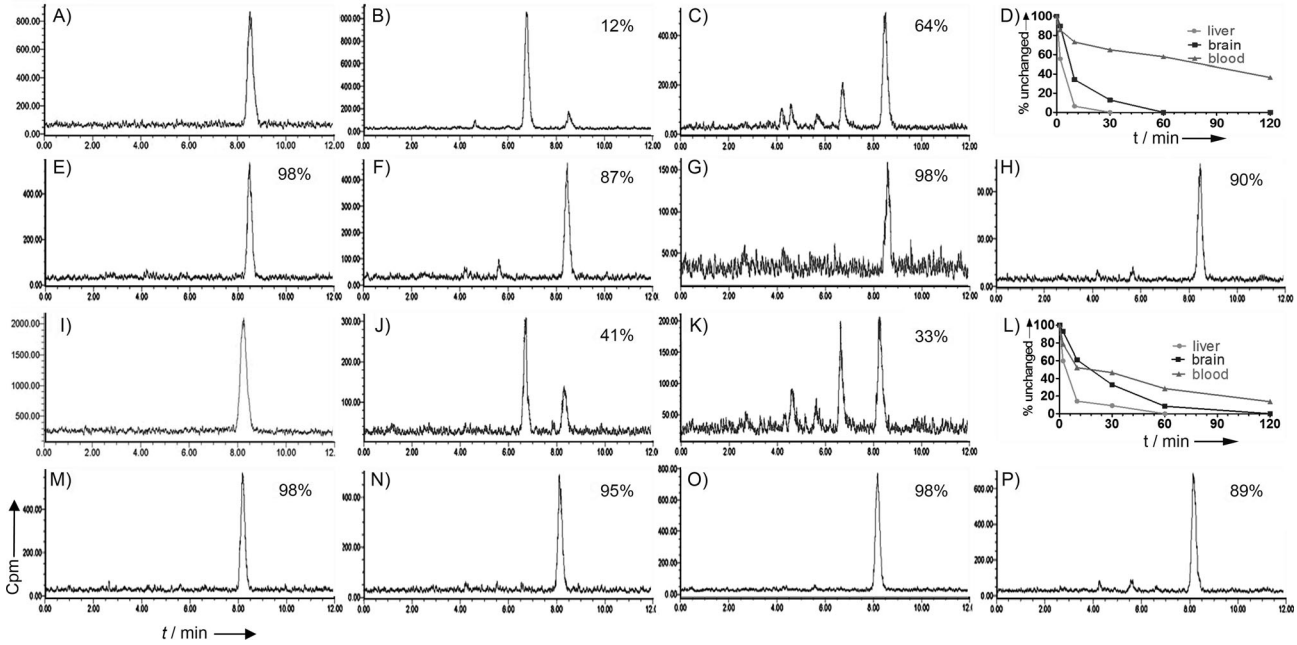

Figure 4. In vitro stabilities of [^{125}I]**2i** and [^{125}I]**2j** in the ICR mouse whole blood, brain, and liver homogenate and in human AD and control brain homogenates. The contents of the images are as follows: A)–H) [^{125}I]**2i**, I)–P) [^{125}I]**2j**, A) and I) purified [^{125}I]**2i** and [^{125}I]**2j**, B) and J) mouse brain homogenate 30 min, C) and K) mouse whole blood 30 min, together with human AD brain homogenate E) and M) 60 min, and F) and N) 120 min, and human control brain homogenate G) and O) 60 min, and H) and P) 120 min. D) and L) represent the statistical curves of [^{125}I]**2i** and [^{125}I]**2j**, respectively, in the mouse whole blood, liver, and brain homogenate at 2 to 120 min after incubation. The percentage count in the box is the ratio of the unchanged radiolabeled compound after incubation. HPLC parameters: Waters Symmetry C18 analytical column (4.6×250 mm, 5 μm); mobile phase: MeOH/H_2O 9:1; flow rate = 1.0 mL min^{-1}; UV detector at 260 nm. Retention times: t_R = 8.4 min for **2i** (UV) and t_R = 8.5 min for [^{125}I]**2i** (γ), t_R = 8.2 min for **2j** (UV) and t_R = 8.3 min for [^{125}I]**2j** (γ).

Table 2. Biodistributions of [^{125}I]**2i** and [^{125}I]**2j** (% ID g^{-1}, n = 5, means ± SDs) in normal mice after intravenous injection, together with log P values.

Organ	2 min	10 min	30 min	1 h	2 h	6 h	24 h
[^{125}I]**2i** (log P = 2.80)							
blood	4.57 ± 0.14	2.34 ± 0.36	1.51 ± 0.33	1.10 ± 0.20	1.27 ± 0.13	1.00 ± 0.04	0.26 ± 0.08
brain	2.74 ± 0.19	2.16 ± 0.25	0.83 ± 0.17	0.40 ± 0.06	0.22 ± 0.05	0.09 ± 0.01	0.03 ± 0.02
heart	9.07 ± 1.22	2.72 ± 0.45	1.13 ± 0.18	0.76 ± 0.14	0.81 ± 0.30	0.37 ± 0.06	0.10 ± 0.03
liver	25.39 ± 3.78	16.06 ± 1.76	10.92 ± 2.61	6.45 ± 1.30	6.05 ± 1.17	5.47 ± 1.79	1.54 ± 0.22
spleen	4.19 ± 0.87	2.06 ± 0.45	1.10 ± 0.10	0.91 ± 0.20	0.89 ± 0.22	0.61 ± 0.21	0.12 ± 0.02
lung	16.13 ± 1.83	7.42 ± 1.65	3.39 ± 0.79	2.71 ± 0.51	2.37 ± 0.44	1.52 ± 0.64	0.39 ± 0.13
kidney	10.33 ± 1.05	4.33 ± 0.61	4.17 ± 0.57	2.52 ± 0.80	2.04 ± 0.04	1.31 ± 0.46	0.30 ± 0.09
skin	1.61 ± 0.59	2.40 ± 0.45	1.93 ± 0.32	1.63 ± 0.53	2.36 ± 0.30	0.84 ± 0.21	0.21 ± 0.06
muscle	2.76 ± 0.07	2.28 ± 0.40	1.04 ± 0.15	0.73 ± 0.16	0.69 ± 0.14	0.35 ± 0.06	0.06 ± 0.02
bone	2.53 ± 0.16	1.45 ± 0.37	0.76 ± 0.17	0.54 ± 0.09	0.50 ± 0.13	0.39 ± 0.17	0.13 ± 0.04
[^{125}I]**2j** (log P = 2.57)							
blood	11.31 ± 1.96	9.39 ± 1.63	3.95 ± 0.44	2.99 ± 0.31	2.31 ± 0.41	1.15 ± 0.16	0.84 ± 0.26
brain	4.58 ± 0.42	3.35 ± 0.38	0.75 ± 0.08	0.45 ± 0.02	0.32 ± 0.04	0.15 ± 0.02	0.09 ± 0.02
heart	10.64 ± 1.35	6.20 ± 1.40	2.29 ± 0.42	1.48 ± 0.12	1.21 ± 0.17	0.68 ± 0.09	0.39 ± 0.07
liver	28.12 ± 3.29	26.34 ± 3.89	14.84 ± 1.68	11.18 ± 1.90	9.12 ± 1.72	7.30 ± 1.18	2.40 ± 0.46
spleen	5.73 ± 0.43	4.98 ± 0.66	1.64 ± 0.04	1.41 ± 0.16	1.10 ± 0.13	0.76 ± 0.09	0.57 ± 0.07
lung	16.15 ± 2.15	11.33 ± 2.94	4.45 ± 0.67	2.85 ± 0.44	2.52 ± 0.16	1.78 ± 0.18	0.84 ± 0.11
kidney	15.12 ± 2.10	14.12 ± 3.92	10.98 ± 3.47	8.50 ± 1.15	6.63 ± 2.25	2.24 ± 0.45	0.80 ± 0.17
skin	4.24 ± 0.96	5.33 ± 1.20	3.6 ± 0.81	2.58 ± 0.38	1.81 ± 0.44	1.22 ± 0.32	0.43 ± 0.13
muscle	4.57 ± 0.68	3.07 ± 0.43	1.25 ± 0.20	1.47 ± 0.46	1.03 ± 0.38	0.63 ± 0.17	0.20 ± 0.03
bone	4.20 ± 0.65	3.36 ± 0.54	1.48 ± 0.16	1.29 ± 0.19	0.75 ± 0.25	0.46 ± 0.09	0.32 ± 0.07

the more flexible design offers extra substituent groups for labeling with ^{11}C or ^{18}F, such as **2k** or **2e.**

Taken together, the primary results of this study provide a structure scaffold for the design of compounds able to bind to Aβ with high affinities and suitable for development as in vivo imaging agents for Aβ plaques.

Experimental Section

Materials and instruments: The reagents used in the syntheses were purchased from Alfa Aesar, Sigma–Aldrich, and Sinopharm Chemical Reagent Co. Ltd and were used without further purification unless otherwise indicated. Compound **1** was prepared as described previously.[29] [^{125}I]NaI (2200 Ci mmol^{-1}) was purchased from

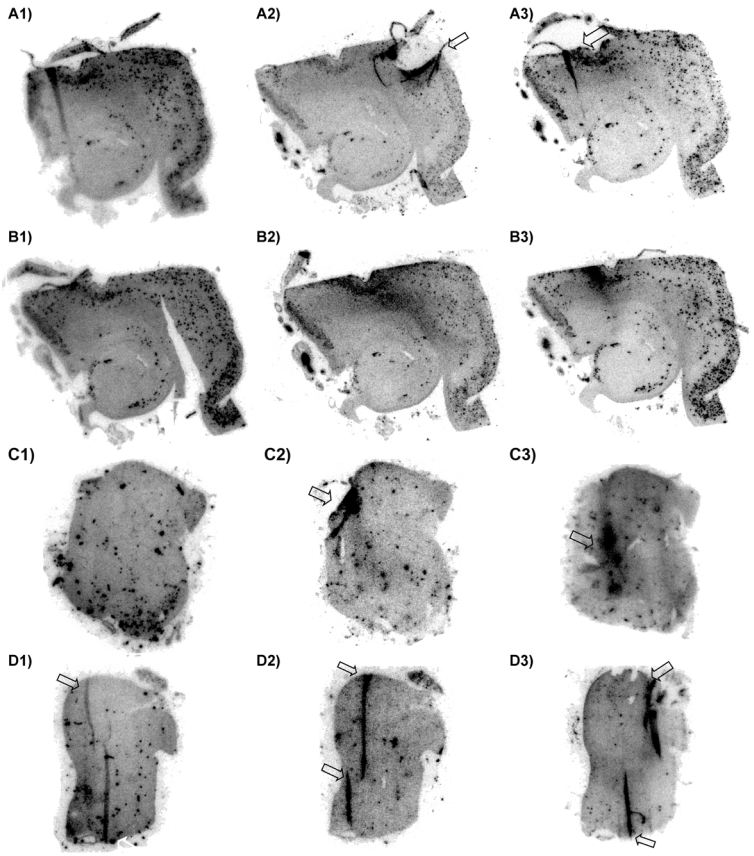

Figure 5. Autoradiography of human brain sections. The top two rows (A, B) contain sections of human AD (91-year old female, Braak 5, temporal cortex), the bottom two rows (C, D) contain sections of human control brains (C: 72-year old female, Braak 0, hippocampus. D: 69-year old female, Braak 1, hippocampus). Columns 1–3 are sections labeled with [^{125}I]**1**,[^{125}I]**2i**, and [^{125}I]**2j**, respectively. In the AD brain sections, many SPs were labeled by [^{125}I]**2i** (A2, B2) and [^{125}I]**2j** (A3, B3), relative to those by [^{125}I]**1** (A1, B1). In the control brain sections, just a few SPs were labeled by [^{125}I]**2i** (C2, D2) and [^{125}I]**2j** (C3, D3), with images similar to those provided by [^{125}I]**1** (C1, D1). The solid arrows indicate thick and abnormal silver particles due to bubbles or creases in the tissue sections.

Perkin–Elmer Life and Analytical Sciences (USA). The AD human brain homogenates and paraffin brain sections were obtained from the Netherlands brain bank (coordinator: Dr. Inge Huitinga); permission was obtained for the use of the tissue and clinical information for research purposes. The ^{1}H NMR spectra were obtained with a Bruker Avance-500 (500 MHz) spectrometer with TMS as the internal standard. High-resolution MS were obtained with Micromass GCT (EI-MS, for compounds **2a**–**j**) and Thermo Electron ProteomeX LTQ instruments (ESI-MS, for compounds **2k**–**m**). Elemental analyses were obtained with an Elementar Vario EL III system. FTIR spectra were obtained with a Thermo Scientific Nicolet 8700 system. Melting points were determined by use of a YRT-3 apparatus and capillary tubes and were uncorrected. All key compounds were found to be of $\geq$95% purity by elemental analysis. The HPLC system consisted of a Waters 1525 binary high-pressure gradient pump, a 2489 variable dual wavelength ultraviolet (UV) detector, a Bioscan Flow-Count FC-3100 NaI PMT based radioactivity detector, and Hamilton manual glass injectors.

(*E*)-2-Benzylidene-5,6-dimethoxyindan-1-one (2a): Indanone **3a** (192 mg, 1.0 mmol) and benzaldehyde **4a** (106 mg, 1.0 mmol) were dissolved in ethanol (10 mL). Aqueous NaOH solution (10%) was added to this solution dropwise with stirring. The reaction was conducted overnight at room temperature. The precipitate was filtered to produce a yellow solid, which was recrystallized from ethanol to give **2a** (241 mg, 86%) as a pale yellow solid. M.p. 184–186 °C; ^{1}H NMR ($CDCl_3$): δ = 7.66–7.64 (m, 2H; H-2′, H-6′), 7.59 (s, 1H; =CHPh), 7.46–7.43 (m, 2H; H-3′, H-5′), 7.40–7.37 (m, 1H; H-4′), 7.33 (s, 1H; H-7), 6.98 (s, 1H; H-4), 4.00 (s, 3H; OCH_3), 3.96 (s, 2H; H-3), 3.95 ppm (s, 3H; OCH_3); ^{13}C NMR ($CDCl_3$): δ = 193.3, 155.6, 149.8, 145.1, 135.7, 135.6, 132.6, 131.2, 130.7, 129.5, 129.2, 129.1, 129.0, 107.3, 105.2, 56.5, 56.3, 32.3 ppm; IR (KBr): $\tilde{\nu}$ = 3002, 2938, 2835, 1688, 1631, 1587, 1501, 1305, 1255, 1223, 1128, 1095, 774 cm^{-1}; HRMS: calcd for $C_{18}H_{16}O_3$: 280.1099 $[M]^+$; found: 280.1092; elemental analysis calcd (%) for $C_{18}H_{16}O_3$: C 77.12, H 5.75; found: C 76.61, H 5.82.

(*E*)-2-(4-Bromobenzylidene)-5,6-dimethoxyindan-1-one (2b): Compound **2b** (294 mg, 82%) was prepared from **3a** (192 mg, 1 mmol) and **4b** (185 mg, 1 mmol), in a procedure similar to that described for compound **2a**, as a white solid. M.p. 178–180 °C; ^{1}H NMR ($CDCl_3$): δ = 7.57–7.55 (m, 2H; H-3′, H-5′), 7.49–7.47 (m, 3H; H-2′, H-6′, = CHPh), 7.30 (s, 1H; H-7), 6.96 (s, 1H; H-4), 3.99 (s, 3H; OCH_3), 3.94 (s, 3H; OCH_3), 3.89 ppm (s, 2H; H-3); ^{13}C NMR ($CDCl_3$): δ = 193.0, 155.7, 149.8, 144.9, 136.2, 134.6, 132.3, 132.2, 132.0, 131.9, 131.8, 131.1, 123.9, 107.2, 105.2, 56.5, 56.3, 32.3 ppm; IR (KBr): $\tilde{\nu}$ = 3003, 2938, 2834, 1690, 1632, 1585, 1500, 1309, 1128, 1090, 1007, 796 cm^{-1}; HRMS: calcd for $C_{18}H_{15}{}^{79}BrO_3$: 358.0205 $[M]^+$; found: 358.0203; HRMS: calcd for $C_{18}H_{15}{}^{81}BrO_3$: 360.0184 $[M]^+$; found: 360.0175; elemental analysis calcd (%) for $C_{18}H_{15}BrO_3$: C 60.18, H 4.21; found: C 60.40, H 4.21.

(*E*)-5,6-Dimethoxy-2-(4-nitrobenzylidene)indan-1-one (2c): Compound **2c** (289 mg, 89%) was prepared from **3a** (192 mg, 1.0 mmol) and **4c** (151 mg, 1.0 mmol), in a procedure similar to that described for compound **2a**, as a yellow solid. M.p. 211–213 °C; ^{1}H NMR ($CDCl_3$): δ = 8.31 (d, J = 8.7 Hz, 2H; H-3′, H-5′), 7.79 (d, J = 8.7 Hz, 2H; H-2′, H-6′), 7.61 (s, 1H; =CHPh), 7.36 (s, 1H; H-7), 7.00 (s, 1H; H-4), 4.02 (s, 3H; OCH_3), 4.01 (s, 2H; H-3), 3.96 ppm (s, 3H; OCH_3); ^{13}C NMR ($CDCl_3$): δ = 192.3, 156.1, 150.0, 147.6, 144.8, 141.9, 139.3, 130.8, 129.4, 124.1, 107.2, 105.3, 56.4, 56.2, 32.1 ppm; IR (KBr): $\tilde{\nu}$ = 3077, 2944, 2866, 1682, 1631, 1516, 1502, 1341, 1310, 1095, 1002, 850 cm^{-1}; HRMS: calcd for $C_{18}H_{15}NO_5$: 325.0950 $[M]^+$; found: 325.0947; elemental analysis calcd (%) for $C_{18}H_{15}NO_5$: C 66.46, H 4.65, N 4.31; found: C 65.60, H 4.53, N 4.24.

(*E*)-2-(4-Aminobenzylidene)-5,6-dimethoxyindan-1-one (2d): Tin(II) chloride dihydrate (695 mg, 3.08 mmol) was added to a solution of 5,6-dimethoxy-2-(4-nitrobenzylidene)indan-1-one (**2c**, 200 mg, 0.61 mmol) in ethanol (25 mL). The reaction mixture was heated at reflux under nitrogen for 4 h and then allowed to cool to room temperature. Ethanol was evaporated off, and NaOH (1 M) was added until the mixture became basic (pH 8–9). After extraction with ethyl acetate (50 mL×2), the combined organic layers were washed with brine, dried over anhydrous Na_2SO_4, and filtered. The solvent was removed, and the residue was purified by silica gel chromatography (petroleum ether/ethyl acetate 2:1) to produce **2d** (92 mg, 56%) as a pale brown solid. M.p. 223–225 °C; ^{1}H NMR ($CDCl_3$): δ = 7.52–7.48 (m, 3H; H-2′, H-6′, =CHPh), 7.34 (s, 1H; H-7), 6.97 (s, 1H; H-4), 6.74–6.71 (m, 2H; H-3′, H-5′), 3.99 (s, 3H; OCH_3), 3.94 (s, 3H; OCH_3), 3.91 ppm (s, 2H; H-3); ^{13}C NMR ($CDCl_3$): δ = 193.5, 144.7, 133.2, 132.7, 115.3, 107.3, 105.1, 56.4, 56.3,

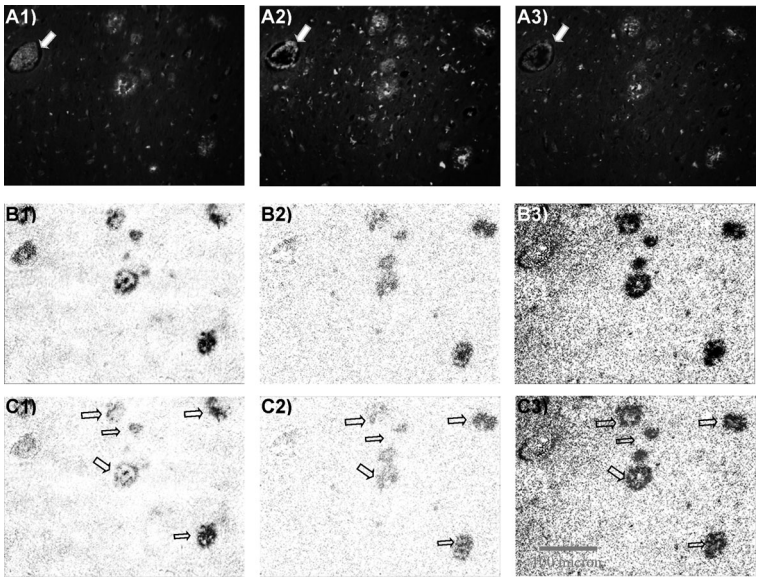

Figure 6. Autoradiography of human AD brain sections (91-year old female, Braak 5, temporal cortex). Columns 1–3: sections labeled with [^{125}I]**1**,[^{125}I]**2i**, and [^{125}I]**2j**, respectively. Rows A–C represent images from the ThS fluorescent staining and in situ micro-autoradiography, as well as the merged images. The white solid arrows indicate the landmarks. The black hollow arrows indicate SPs. The SPs are labeled by [^{125}I]**2i** (B2) or [^{125}I]**2j** (C2), and the images are comparable to those labeled by [^{125}I]**1** (A2). Furthermore, the senile plaques are co-labeled by ThS and merged with the silver particles very well (C1, C2, C3). Scale bar = 100 μm.

32.5 ppm; IR (KBr): $\tilde{\nu}$ = 3427, 3348, 2929, 1671, 1578, 1499, 1304, 1130, 1099, 1004, 819 cm^{-1}; HRMS: calcd for $C_{18}H_{17}NO_3$: 295.1208 $[M]^+$; found: 295.1201; elemental analysis calcd (%) for $C_{18}H_{17}NO_3$: C 73.20, H 5.80, N 4.74; found: C 72.12, H 5.95, N 4.53.

(*E*)-2-[4-(Dimethylamino)benzylidene]-5,6-dimethoxyindan-1-one (2e): Compound **2e** (258 mg, 80%) was prepared from **3a** (192 mg, 1.0 mmol) and **4d** (149 mg, 1.0 mmol), in a procedure similar to that described for compound **2a**, as a light brown solid. M.p. 206–208 °C; ^{1}H NMR ($CDCl_3$): δ = 7.59–7.57 (m, 3H; H-2′, H-6′, =CHPh), 7.34 (s, 1H; H-7), 6.98 (s, 1H; H-4), 6.75–6.73 (m, 2H; H-3′, H-5′), 3.99 (s, 3H; OCH_3), 3.95 (s, 3H; OCH_3), 3.92 (s, 2H; H-3), 3.05 ppm (s, 6H; NMe_2); ^{13}C NMR ($CDCl_3$): δ = 193.4, 154.6, 150.9, 149.3, 144.3, 133.4, 132.4, 131.6, 130.5, 123.3, 111.9, 107.1, 104.9, 56.2, 56.1, 40.1, 32.3 ppm; IR (KBr): $\tilde{\nu}$ = 2923, 1676, 1596, 1524, 1303, 1122, 1001, 817 cm^{-1}. HRMS: calcd for $C_{20}H_{21}NO_3$: 323.1521 $[M]^+$; found: 323.1513; elemental analysis calcd (%) for $C_{20}H_{21}NO_3$: C 74.28, H 6.55, N 4.33; found: C 72.33, H 6.42, N 4.63.

(*E*)-5,6-Dimethoxy-2-(4-methoxybenzylidene)indan-1-one (2f): Compound **2f** (242 mg, 78%) was prepared from **3a** (192 mg, 1.0 mmol) and **4e** (136 mg, 1.0 mmol), in a procedure similar to that described for compound **2a**, as a yellow solid. M.p. 188–190 °C; ^{1}H NMR ($CDCl_3$): δ = 7.63–7.62 (d, J = 8.6 Hz, 2H; H-2′, H-6′), 7.57 (s, 1H; =CHPh), 7.35 (s, 1H; H-7), 6.99–6.97 (m, 3H; H-3′, H-5′, H-4), 3.99 (s, 3H; OCH_3), 3.95–3.94 (m, 5H; OCH_3, H-3), 3.87 ppm (s, 3H; OCH_3); ^{13}C NMR ($CDCl_3$): δ = 193.3, 160.6, 155.2, 149.5, 144.7, 133.1, 132.3, 131.2, 128.3, 114.4, 107.2, 105.0, 56.3, 56.2, 55.4, 32.2 ppm; IR (KBr): $\tilde{\nu}$ = 2941, 2834, 1685, 1605, 1504, 1299, 1258, 1091, 820 cm^{-1}; HRMS: calcd for $C_{12}H_{18}O_4$: 310.1205 $[M]^+$; found: 310.1202; elemental analysis calcd (%) for $C_{12}H_{18}O_4$: C 73.53, H 5.85; found: C 70.27, H 5.58.

(*E*)-5-Bromo-2-[4-(dimethylamino)benzylidene]indan-1-one (2g): Compound **2g** (256 mg, 75%) was prepared from **3b** (211 mg, 1.0 mmol) and **4d** (149 mg, 1.0 mmol), in a procedure similar to that described for compound **2a**, as a brown solid. M.p. 218–220 °C; ^{1}H NMR ($CDCl_3$): δ = 7.75–7.64 (m, 3H; H-7, H-6, H-4), 7.58–7.53 (m, 3H; = CHPh, H-2′, H-6′), 6.74–6.71 (m, 2H; H-3′, H-5′), 3.95 (s, 2H; H-3), 3.05 ppm (s, 6H; NMe_2); ^{13}C NMR ($CDCl_3$): δ = 193.0, 151.3, 151.0, 137.7, 135.7, 132.9, 130.9, 129.2, 128.9, 128.6, 125.2, 122.8, 111.9, 40.0, 32.4 ppm; IR (KBr): $\tilde{\nu}$ = 2919, 1683, 1592, 1526, 1444, 1316, 1113, 960, 882 cm^{-1}; HRMS: calcd for $C_{18}H_{16}{}^{79}BrNO$: 341.0415 $[M]^+$; found: 341.0417; HRMS: calcd for $C_{18}H_{16}{}^{81}BrNO$: 343.0395 $[M]^+$; found: 343.0392; elemental analysis calcd (%) for $C_{18}H_{16}BrNO$: C 63.17, H 4.71, N 4.09; found: C 61.69, H 4.54, N 3.94.

(*E*)-6-Bromo-2-[4-(dimethylamino)benzylidene]indan-1-one (2h): Compound **2h** (263 mg, 77%) was prepared from **3c** (211 mg, 1.0 mmol) and **4d** (149 mg, 1.0 mmol), in a procedure similar to that described for compound **2a**, as a brown solid. M.p. 192–194 °C; ^{1}H NMR ($CDCl_3$): δ = 8.00 (s, 1H; H-7), 7.67–7.64 (m, 2H; H-5, =CHPh), 7.57 (d, J = 8.8 Hz, 2H; H-2′, H-6′), 7.41 (d, J = 8.0 Hz, 1H; H-4), 6.72 (d, J = 8.8 Hz, 2H; H-3′, H-5′), 3.91 (s, 2H; H-3), 3.06 ppm (s, 6H; NMe_2); ^{13}C NMR ($CDCl_3$): δ = 193.0, 151.5, 148.0, 140.9, 136.6, 136.2, 133.2, 129.4, 127.7, 127.2, 123.0, 121.8, 112.0, 40.3, 32.6 ppm; IR (KBr): $\tilde{\nu}$ = 2893, 1681, 1589, 1523, 1462, 1363, 1188, 1169, 1115, 810 cm^{-1}; HRMS: calcd for $C_{18}H_{16}{}^{79}BrNO$ $[M]^+$ 341.0415; found: 341.0409; HRMS: calcd for $C_{18}H_{16}{}^{81}BrNO$: 343.0395 $[M]^+$; found: 343.0387; elemental analysis calcd (%) for $C_{18}H_{16}BrNO$: C 63.17, H 4.71, N 4.09; found: C 62.58, H 4.63, N 3.98.

(*E*)-2-[4-(Dimethylamino)benzylidene]-5-iodoindan-1-one (2i): A solution of iodine (53 mg, 0.20 mmol) in THF (2 mL) was added dropwise to a cooled (ice bath) solution of **2n** (75 mg, 0.14 mmol) in THF (3 mL). After the addition, the mixture was stirred at 0 °C for 1 h and the reaction was terminated by the addition of saturated $NaHSO_3$ solution (5 mL). The reaction mixture was extracted with ethyl acetate (3×10 mL) after neutralization with saturated $NaHCO_3$ solution (5 mL). The combined organic layers were dried over Na_2SO_4 and filtered. The solvent was removed, and the residue was purified by silica gel chromatography (petroleum ether/ethyl acetate 6:1) to produce **2i** (42 mg, 77%) as a brown solid. M.p. 203–205 °C; ^{1}H NMR ($CDCl_3$): δ = 7.95 (s, 1H; H-4), 7.77 (m, 1H; H-6), 7.66 (s, 1H; =CHPh), 7.62–7.58 (m, 3H; H-2′, H-6′, H-7), 6.78 (d, J = 7.9 Hz, 2H; H-3′, H-5′), 3.96 (s, 2H; H-3), 3.07 ppm (s, 6H; NMe_2); ^{13}C NMR ($CDCl_3$): δ = 193.6, 151.1, 138.4, 137.0, 135.9, 135.5, 133.1, 125.5, 112.4, 101.9, 40.5, 32.4 ppm; IR (KBr): $\tilde{\nu}$ = 2898, 1682, 1590, 1525, 1312, 1111, 959, 810 cm^{-1}; HRMS: calcd for $C_{18}H_{16}INO$: 389.0277 $[M]^+$; found: 389.0271; elemental analysis calcd (%) for $C_{18}H_{16}INO$: C 55.54, H 4.14, N 3.60; found: C 52.86, H 3.96, N 3.42.

(*E*)-2-[4-(Dimethylamino)benzylidene]-6-iodoindan-1-one (2j): Compound **2j** (295 mg, 76%) was prepared from **3d** (258 mg, 1.0 mmol) and **4d** (149 mg, 1 mmol), in a procedure similar to that described for compound **2a**, as a brown solid. M.p. 223–225 °C; ^{1}H NMR ($CDCl_3$): δ = 8.20 (s, 1H; H-7), 7.85–7.83 (m, 1H; H-5), 7.63 (s, 1H; =CHPh), 7.55 (d, J = 8.8 Hz, 2H; H-2′, H-6′), 7.30–7.26 (m, 1H; H-4), 6.71 (d, J = 8.8 Hz, 2H; H-3′, H-5′), 3.88 (s, 2H; H-3), 3.05 ppm (s, 6H; NMe_2); ^{13}C NMR ($CDCl_3$): δ = 192.9, 151.5, 148.7, 142.3, 141.1, 136.1, 133.3, 133.1, 129.1, 128.0, 123.0, 112.1, 92.9, 40.3, 32.6 ppm; IR (KBr): $\tilde{\nu}$ = 2851, 1678, 1585, 1522, 1362, 1308, 1263, 1187, 1116, 809 cm^{-1}; HRMS: calcd for $C_{18}H_{16}INO$: 389.0277

$[M]^+$; found: 389.0279; elemental analysis calcd (%) for $C_{18}H_{16}INO$: C 55.54, H 4.14, N 3.60; found: C 52.71, H 4.07, N 3.36.

(*E*)-2-[4-(Dimethylamino)benzylidene]-5-methoxyindan-1-one (2k): Compound **2k** (249 mg, 85%) was prepared from **3e** (162 mg, 1.0 mmol) and **4d** (149 mg, 1 mmol), in a procedure similar to that described for compound **2a**, as a light brown solid. M.p. 204–205 °C; ^{1}H NMR ($CDCl_3$): δ = 7.83 (d, J = 8.4 Hz, 1H; H-7), 7.59–7.56 (m, 3H; H-2′, H-6′, =CHPh), 6.99 (m, 1H; H-4), 6.96–6.92 (dd, J = 8.4 Hz, 1.8 Hz, 1H; H-6), 6.74 (d, J = 8.7 Hz, 2H; H-3′, H-5′), 3.95 (s, 2H; H-3), 3.90 (s, 3H; OCH_3), 3.05 ppm (s, 6H; NMe_2); ^{13}C NMR ($CDCl_3$): δ = 193.0, 164.7, 152.2, 151.0, 133.7, 132.5, 132.1, 130.4, 125.7, 123.3, 114.8, 111.9, 109.7, 55.6, 40.1, 32.8 ppm; IR (KBr): $\tilde{\nu}$ = 3441, 2995, 2935, 1675, 1579, 1544, 1303, 1120 cm^{-1}; HRMS: calcd for $C_{19}H_{19}NO_2$: 293.1416 $[M+H]^+$; found: 294.1491; elemental analysis calcd (%) for $C_{19}H_{19}NO_2$: C 77.79, H 6.53, N 4.77; found: C 76.59, H 6.56, N 4.73.

(*E*)-2-[4-(Dimethylamino)benzylidene]-5-hydroxyindan-1-one (2l): Concentrated HCl (0.38 mL) was added to a suspension of 5-hydroxyindan-1-one (**3f**, 200 mg, 1.35 mmol) in acetic acid (2.1 mL), followed after 10 min of stirring at room temperature by 4-(dimethylamino)benzaldehyde (**4d**, 201 mg, 1.35 mmol). The mixture was stirred for 2 h at room temperature, allowed to stand for 2 days, and made basic with saturated aqueous Na_2CO_3. The resulting precipitate was collected and purified by column chromatography on silica gel (CH_2Cl_2/methanol 20:1) to produce **2l** (244 mg, 65%) as a brown solid. M.p. 252–255 °C; ^{1}H NMR ([D$_6$]DMSO): δ = 7.58–7.53 (m, 3H; H-7, H-2′, H-6′), 7.29 (s, 1H; =CHPh), 6.87 (s, 1H; H-4), 6.80–6.75 (m, 3H; H-6, H-3′, H-5′), 3.88 (s, 2H; H-3), 3.63 (br, 1H; OH), 3.00 ppm (s, 6H; NMe_2); ^{13}C NMR ([D$_6$]DMSO): δ = 190.9, 166.1, 152.5, 150.7, 132.1, 131.5, 131.3, 130.9, 128.4, 125.3, 122.7, 116.6, 112.1, 111.0, 40.1, 32.0 ppm; IR (KBr): $\tilde{\nu}$ = 3151, 2892, 1666, 1577, 1526, 1296, 1189, 1091 cm^{-1}; HRMS: calcd for $C_{18}H_{17}NO_2$: 279.1259 $[M+H]^+$; found: 280.1330; elemental analysis calcd (%) for $C_{18}H_{17}NO_2$: C 77.40, H 6.13, N 5.01; found: C 75.75, H 6.21, N 4.89.

(*E*)-2-[3-Bromo-4-(dimethylamino)benzylidene]-5,6-dimethoxyindan-1-one (2m): Compound **2m** (305 mg, 76%) was prepared from **3a** (192 mg, 1.0 mmol) and 3-bromo-4-(dimethylamino)benzaldehyde (228 mg, 1.0 mmol), in a procedure similar to that described for compound **2a**, as a yellow solid. M.p. 157–159 °C; ^{1}H NMR ($CDCl_3$): δ = 7.88 (d, J = 1.8 Hz, 1H; H-2′), 7.53 (dd, J = 1.8 Hz, 8.4 Hz, 1H; H-6′), 7.48 (s, 1H; =CHPh), 7.34 (s, 1H; H-7), 7.09 (d, J = 8.4 Hz, 1H; H-5′), 7.01 (s, 1H; H-4), 4.01 (s, 3H; OCH_3), 3.96 (s, 3H; OCH_3), 3.95 (s, 2H; H-3), 2.89 ppm (s, 6H; NMe_2); ^{13}C NMR ($CDCl_3$): δ = 192.9, 155.4, 152.6, 149.7, 144.6, 136.0, 135.7, 134.5, 131.1, 130.9 (2C), 130.7, 120.1, 118.2, 107.2, 105.1, 56.3, 56.2, 43.8, 32.0 ppm; IR (KBr): $\tilde{\nu}$ = 3439, 2939, 2881, 1692, 1591, 1503, 1303, 1124 cm^{-1}; HRMS: calcd for $C_{20}H_{20}{}^{79}BrNO_3$: 401.0627 $[M+Na]^+$; found: 424.0517; HRMS: calcd for $C_{20}H_{20}{}^{81}BrNO_3$: 403.0606 $[M+Na]^+$; found: 426.0497; elemental analysis calcd (%) for $C_{20}H_{20}BrNO_3$: C 59.71, H 5.01, N 3.48; found: C 56.81, H 4.73, N 3.33.

(*E*)-2-[4-(Dimethylamino)benzylidene]-5-(tributylstannyl)indan-1-one (2n): A mixture of **2g** (400 mg, 1.17 mmol), bis(tributyltin) (4.0 g, 7.02 mmol), and $Pd(PPh_3)_4$ (135 mg, 0.12 mmol) in Et_3N (15 mL) was stirred at 80 °C under nitrogen for 16 h. The solvent was removed, and the residue was purified by silica gel chromatography (petroleum ether/ethyl acetate 8:1) to produce **2n** (176 mg, 27%) as a brown oil; ^{1}H NMR ($CDCl_3$): δ = 7.82 (d, J = 7.5 Hz, 1H; H-7), 7.68–7.64 (m, 2H; =CHPh, H-4), 7.62–7.59 (d, J = 9.0 Hz, 2H; H-2′, H-6′), 7.52 (d, J = 7.5 Hz, 1H; H-6), 6.75–6.72 (d, J = 9.0 Hz, 2H; H-3′, H-5′), 3.99 (s, 2H; H-3), 3.04 (s, 6H; NMe_2), 1.61–1.51 (m, 6H; $SnBu_3$), 1.41–1.29 (m, 6H; $SnBu_3$), 1.14–1.08 (m, 6H; $SnBu_3$), 0.92–0.90 ppm (t, J = 7.2 Hz, 9H; $SnBu_3$); IR (film): $\tilde{\nu}$ = 2955, 2925, 1687, 1624, 1595, 1453, 1091, 882 cm^{-1}; MS (ESI): *m/z*: 528.28 $[M+H]^+$.

(*E*)-2-[4-(Dimethylamino)benzylidene]-6-(tributylstannyl)indan-1-one (2o): Compound **2o** (106 mg, 33%) was prepared from **2h** (200 mg, 0.59 mmol), in a procedure similar to that described for compound **2n**, as a brown oil; ^{1}H NMR ($CDCl_3$): δ = 8.01 (s, 1H; H-7), 7.66–7.64 (m, 2H; H-5, H-4), 7.61–7.58 (d, J = 9.0 Hz, 2H; H-2′, H-6′), 7.53 (s, 1H; =CHPh), 6.75–6.72 (d, J = 9.0 Hz, 2H; H-3′, H-5′), 3.97 (s, 2H; H-3), 3.04 (s, 6H; NMe_2), 1.58–1.49 (m, 6H; $SnBu_3$), 1.37–1.30 (m, 6H; $SnBu_3$), 1.13–1.07 (m, 6H; $SnBu_3$), 0.91–0.89 ppm (t, J = 7.2 Hz, 9H; $SnBu_3$); IR (film): $\tilde{\nu}$ = 2925, 1735, 1686, 1596, 1524, 1458, 1109, 882 cm^{-1}.

Preparation of radioiodinated ligands: The radioiodinated ligands [^{125}I]**2i**, [^{125}I]**2j**, and [^{125}I]**1** were prepared through iododestannylation reactions from the corresponding tributyltin precursors (**2n**, **2o**, and the tributyltin precursor of [^{125}I]**1**) by the methods described previously.[26,47,48] A solution of H_2O_2 (3%, *w/v*, 100 μL) was added to a mixture of the tributyltin precursor solution (100 μg in 100 μL of EtOH), HCl (1 N, 100 μL), and no-carrier-added [^{125}I]NaI solution (1–2 mCi, specific activity of 2200 Ci mmol^{-1}) in a sealed vial. The reaction was conducted at room temperature (25 °C) for 10 min and terminated by the addition of saturated $NaHSO_3$ solution (200 μL). After neutralization with saturated $NaHCO_3$ solution, the reaction mixture was extracted with ethyl acetate (3×1 mL, chromatographically pure). The combined organic extracts were dried by blowing with a stream of nitrogen gas. The residue was redissolved in MeOH (0.4 mL) and purified by reversed-phase HPLC (column: Waters Symmetry C18, 4.6×250 mm, 5 μm; mobile phase: MeOH/H_2O 9:1 for [^{125}I]**2i** and [^{125}I]**2j**, or 8:2 for [^{125}I]**1**; flow rate = 1.0 mL min^{-1}). The fraction containing the labeled compound was collected and checked for radiochemical purity by analytical HPLC and for identity by co-injection with a reference standard. The collected fraction was then dried by blowing with a stream of nitrogen gas, and the residue was redissolved in EtOH (100%) and stored at −20 °C until use. Prior to its use in the animal biodistribution studies, in vitro AD homogenate binding assays, partition coefficient determination, stability study, and autoradiography (ARG) experiments, the radioligand was repurified by dilution with H_2O and passage through a Sep-Pak C18 column. After washing of the column with H_2O (2 mL) and EtOH (30%, 2 mL), the desired products were then eluted either with EtOH (90%, 1 mL, [^{125}I]**2i** or [^{125}I]**2j**) or with EtOH (80%, 1 mL, [^{125}I]**1**).

Preparation of brain tissue homogenates: Several frozen AD brain tissues (stored at −80 °C) were thawed and placed on ice. The gray and white matters were dissected, weighed, and homogenized in ice-cooled phosphate-buffered saline (PBS) solution (0.05 M, pH 7.4) at a concentration of approximately 100 mg wet tissue per mL with the aid of a motor-driven homogenizer (Glas-Col, USA, 30 rpm, 2 min). The homogenates were aliquoted into 1 mL portions and stored at −80 °C. For binding assays, the homogenates were thawed, diluted with ice-cold PBS solution (0.05 M, pH 7.4), and homogenized again with the aid of an ice-cold hand-held glass homogenizer.

In vitro binding assays with AD brain homogenates: Radioligand competition binding assays were conducted in borosilicate glass tubes (12×75 mm, VWR International, USA), by the method described previously, with some modifications.[30,47,49] The AD brain homogenates in PBS (0.05 M, pH 7.4,100 μL), a solution of the radioligand {[^{125}I]**1**, 0.05 nM diluted with PBS/BSA [bovine serum al-

bumin (BSA, 0.1%) in PBS (0.05 M, pH 7.4)], 100 μL}, a solution of the inhibitor ligand [3×10^{-5}–1×10^{-9} M, diluted in a solution containing ethanol (9%) and DMSO (1%) in PBS/BSA, 100 μL], and PBS/BSA (700 μL), for a final volume to 1 mL, were combined in a glass tube. The nonspecific binding was defined in the presence of unlabeled **1** (6×10^{-7} M final concentration, 100 μL) in the same assay tubes. The mixture was incubated at 37 °C in a water bath shaker (60 rpm) for 2 h. The bound and free radioactivity were separated by vacuum filtration through Whatman GF/B filters [immersed with polyethylenimine (PEI, 1%) in PBS on ice] by use of a ZT-II-12R cell harvester (Satellite Medical Equipment, Shaoxing, China) and washed with ice-cold PBS solution (3×3 mL). The filters containing the bound radioligand were counted in a gamma counter (USTC Zonkia GC-1200, Hefei, China) with a 65% counting efficiency. The values for the half-maximum inhibition concentrations (IC_{50}) were computed from the displacement curves of three independent experiments with use of GraphPad Prism 5. In addition, the K_i values were calculated by use of the Cheng–Prusoff equation: $K_i = IC_{50}/(1+[L]/K_d)$,[50] where [L] is the concentration of radioligand used in the assay and K_d is the dissociation constant of the radioligand.

AD brain tissue fluorescent staining: Brain tissues were obtained from several autopsy-confirmed AD subjects. Adjacent tissue sections (6 μm thickness) were processed for staining by the methods described in the literature, with some modifications.[30,47,51] Firstly, the paraffinized brain sections were treated with washes in xylene (2×10 min), washes in EtOH (100%, 2×10 min), sequential washes in EtOH (95, 90, 80 and 70%, 5 min), and sequential rinses (5 min each) in Milli-Q water and PBS (0.01 M, pH 7.4). Secondly, the autofluorescence was quenched as described previously.[47,52] The sections were blanched in potassium permanganate solution (0.25%) for 20 min, washed in PBS, and treated with potassium metabisulfite (0.1%) and oxalic acid (0.1%) in PBS, followed by washing in PBS. The quenched brain tissue sections were immersed in a solution of cold ligand [50 μM diluted in EtOH (30%) in PBS (0.1 M), 20 min], ThS (1% in Milli-Q water, 5 min), or CR [0.5% in EtOH/H_2O (50%), 10 min]. Thirdly, the sections were differentiated with EtOH/H_2O (50%) for 10 min (cold ligand), EtOH/H_2O (70%) for 10 min (ThS), or KOH (0.2%) in EtOH/H_2O (80%) for 10 min (CR). Finally, the sections were washed in PBS (3×5 min) and sealed with glycerin/PBS (80%) and coverslips. The sections were stored at 4 °C in the dark and viewed with an Olympus IX71 fluorescence microscope (Olympus, Tokyo, Japan) and a SPOT digital camera (Diagnostic Instruments, USA).

Determination of partition coefficients: The partition coefficients were measured by mixing ligand [^{125}I]**2i** or [^{125}I]**2j** with 3 g each of octan-1-ol and PBS (0.1 M, pH 7.4) in a test tube. The test tube was vortexed for 3 min at room temperature, followed by centrifugation for 5 min. Several weighed samples (ca. 0.5 g each) drawn from the octan-1-ol and buffer layers were counted in a gamma counter. The partition coefficient was determined by calculating the logarithm of the ratio of cpm g^{-1} of the octan-1-ol to that of PBS. The sample from the octan-1-ol layer was repartitioned until consistent values were obtained. The measurements were performed in triplicate and repeated three times.

Organ biodistribution in normal mice: The animal experiments were performed by the protocol approved by the ethics committee of the School of Life Science, University of Science and Technology of China. A saline solution (0.9%, 100 μL) containing [^{125}I]**2i** or [^{125}I]**2j** (2 μCi) was injected into the tail vein of a male ICR mouse [average weight 20–30 g, fed in specific-pathogen-free (SPF) cages]. The mice ($n=5$ for each time point) were euthanized at predetermined time points (2, 10, 30, 60, 120, 360, and 1440 min). The organs of interest were removed and weighed, and the radioactivity was counted with a gamma counter. The tissue radioactivity concentrations (% ID g^{-1}) were calculated by dividing the sample counts per gram of tissue by the counts from 1% of the initially injected dose (100-fold diluted aliquots of the injected material).

Stability study: The in vitro stabilities of [^{125}I]**2i** or [^{125}I]**2j** were determined by the procedures described in the literature, with minor modifications.[46,53] ICR mice (18–25 g, SPF) were anesthetized by peritoneal injection of pentobarbital sodium (50 mg kg^{-1}). After thoracotomy, blood samples were obtained by cardiac puncture and mixed with heparin (Heaplink, Shenzhen, China). The mice were then perfused with cold saline (0.9%, *w/v*, 40 mL) through the exposed right atrium of the heart while the aorta was severed. The excised brain and liver were homogenized with cold saline as they cooled on ice with use of a motor-driven homogenizer (30 rpm, 2 min). The human AD and control brain homogenates were prepared similarly to the method described above for the receptor binding assay, with some modifications: the gray and white matter were mixed together, the homogenate concentration was higher than that in the binding assay, and saline (0.9%, *w/v*) was used in place of the PBS. The protein concentrations of all the samples were determined by the bicinchoninic acid (BCA) method.[54]

The in vitro stabilities were determined by incubation of purified [^{125}I]**2i** or [^{125}I] **2j** (10 μCi) in solutions of 50 μL mouse whole blood, liver and brain or human AD and control brain homogenates at 37 °C for 2, 10, 30, 60 and 120 min. The proteins were precipitated by addition of MeOH (200 μL), and the MeOH samples were counted in a γ-counter and centrifuged at 13000 rpm for 20 min. The supernatant was analyzed by HPLC (under the same HPLC conditions as described above in the section on the preparation of radioiodinated ligands). The precipitates were measured for radioactivity with a γ-counter to allow calculation of the radioactivity that was recovered from the MeOH.

AD brain sections autoradiography (film and in situ micro-autoradiography): The preparation procedures for ARG of tissue sections (6 μm thickness) were the same as those for the staining experiments above. The tissue sections were incubated with solutions of [^{125}I]**2i**,[^{125}I]**2j**, or [^{125}I]**1** [0.3 nM in PBS (0.05 M, pH 7.4)] at 37 °C for 1 h. The sections labeled with [^{125}I]**1** were processed by procedures described in the literature.[30] Sections labeled with [^{125}I]**2i** or [^{125}I]**2j** were washed with PBS for 30 s and differentiated by washing with EtOH/H_2O (70%) for 5 s and rinsing with Milli-Q water for 1 min. After drying in a fume hood, all labeled sections were affixed to X-ray films (Kodak BioMax MR) and exposed for different lengths of time. When optimal images were obtained, the sections were dipped in an emulsion (Amersham Hypercoat Emulsions, RPN40, USA) for in situ micro-ARG. The exposure times were adjusted to obtain optimal images. Finally, all sections were also stained with ThS or CR, stored at 4 °C in the dark, and viewed by fluorescence microscopy by the procedures described above.

Acknowledgements

We thank Prof. Mei-Ping Kung, Prof. Yi-Yun Huang, Prof. Lin Zhu, Dr. Ming-Qiang Zheng and Dr. Xin-Hong Duan for their technical training, advice, and reviewing. We thank Dr. Shi-Cun Wang for his kind assistance. This work was supported by grants from the Nature Science Foundation of China (81030026) and the Ministry

of Science and Technology of China (2011CB504100). The authors declare no conflict of interest.

Keywords: Alzheimer's disease · amyloid beta-peptides · imaging agents · indanones · senile plaques

[1] H. W. Querfurth, F. M. LaFerla, *New Engl. J. Med.* **2010**, *362*, 329 – 344.
[2] R. Brookmeyer, E. Johnson, K. Ziegler-Graham, H. M. Arrighi, *Alzheimer's Dementia* **2007**, *3*, 186 – 191.
[3] E. D. Roberson, L. Mucke, *Science* **2006**, *314*, 781 – 784.
[4] A. Nordberg, *Lancet Neurol.* **2004**, *3*, 519 – 527.
[5] A. Nordberg, *Front. Neurol. Neurosci.* **2009**, *24*, 47 – 53.
[6] A. Nordberg, *Neuropsychologia* **2008**, *46*, 1636 – 1641.
[7] L. Cai, R. B. Innis, V. W. Pike, *Curr. Med. Chem.* **2007**, *14*, 19 – 52.
[8] K. Shoghi-Jadid, G. W. Small, E. D. Agdeppa, V. Kepe, L. M. Ercoli, P. Siddarth, S. Read, N. Satyamurthy, A. Petric, S.-C. Huang, J. R. Barrio, *Am. J. Geriatr. Psychiatry* **2002**, *10*, 24 – 35.
[9] E. D. Agdeppa, V. Kepe, J. Liu, S. Flores-Torres, N. Satyamurthy, A. Petric, G. M. Cole, G. W. Small, S.-C. Huang, J. R. Barrio, *J. Neurosci.* **2001**, *21*, RC189.
[10] M. Ono, A. Wilson, J. Nobrega, D. Westaway, P. Verhoeff, Z. P. Zhuang, M. P. Kung, H. F. Kung, *Nucl. Med. Biol.* **2003**, *30*, 565 – 571.
[11] N. P. L. G. Verhoeff, A. A. Wilson, S. Takeshita, L. Trop, D. Hussey, K. Singh, H. F. Kung, M.-P. Kung, S. Houle, *Am. J. Geriatr. Psychiatry* **2004**, *12*, 584 – 595.
[12] W. E. Klunk, H. Engler, A. Nordberg, Y. Wang, G. Blomqvist, D. P. Holt, M. Bergström, I. Savitcheva, G.-F. Huang, S. Estrada, B. Ausén, M. L. Debnath, J. Barletta, J. C. Price, J. Sandell, B. J. Lopresti, A. Wall, P. Koivisto, G. Antoni, C. A. Mathis, B. Långström, *Ann. Neurol.* **2004**, *55*, 306 – 319.
[13] C. A. Mathis, Y. Wang, D. P. Holt, G. F. Huang, M. L. Debnath, W. E. Klunk, *J. Med. Chem.* **2003**, *46*, 2740 – 2754.
[14] G. J. O'Keefe, T. H. Saunder, S. Ng, U. Ackerman, H. J. Tochon-Danguy, J. G. Chan, S. Gong, T. Dyrks, S. Lindemann, G. Holl, L. Dinkelborg, V. Villemagne, C. C. Rowe, *J. Nucl. Med.* **2009**, *50*, 309 – 315.
[15] C. C. Rowe, U. Ackerman, W. Browne, R. Mulligan, K. L. Pike, G. O'Keefe, H. Tochon-Danguy, G. Chan, S. U. Berlangieri, G. Jones, K. L. Dickinson-Rowe, H. P. Kung, W. Zhang, M. P. Kung, D. Skovronsky, T. Dyrks, G. Holl, S. Krause, M. Friebe, L. Lehman, S. Lindemann, L. M. Dinkelborg, C. L. Masters, V. L. Villemagne, *Lancet Neurol.* **2008**, *7*, 129 – 135.
[16] W. Zhang, S. Oya, M. P. Kung, C. Hou, D. L. Maier, H. F. Kung, *Nucl. Med. Biol.* **2005**, *32*, 799 – 809.
[17] S. R. Choi, G. Golding, Z. Zhuang, W. Zhang, N. Lim, F. Hefti, T. E. Benedum, M. R. Kilbourn, D. Skovronsky, H. F. Kung, *J. Nucl. Med.* **2009**, *50*, 1887 – 1894.
[18] K. J. Lin, W. C. Hsu, I. T. Hsiao, S. P. Wey, L. W. Jin, D. Skovronsky, Y. Y. Wai, H. P. Chang, C. W. Lo, C. H. Yao, T. C. Yen, M. P. Kung, *Nucl. Med. Biol.* **2010**, *37*, 497 – 508.
[19] D. F. Wong, P. B. Rosenberg, Y. Zhou, A. Kumar, V. Raymont, H. T. Ravert, R. F. Dannals, A. Nandi, J. R. Brasic, W. Ye, J. Hilton, C. Lyketsos, H. F. Kung, A. D. Joshi, D. M. Skovronsky, M. J. Pontecorvo, *J. Nucl. Med.* **2010**, *51*, 913 – 920.
[20] C. Mathis, B. Lopresti, N. Mason, J. Price, N. Flatt, W. Bi, S. Ziolko, S. DeKosky, W. Klunk, *J. Nucl. Med. Meeting Abstract* **2007**, *48*, 56P.
[21] M. Koole, D. M. Lewis, C. Buckley, N. Nelissen, M. Vandenbulcke, D. J. Brooks, R. Vandenberghe, K. Van Laere, *J. Nucl. Med.* **2009**, *50*, 818 – 822.
[22] N. Nelissen, K. Van Laere, L. Thurfjell, R. Owenius, M. Vandenbulcke, M. Koole, G. Bormans, D. J. Brooks, R. Vandenberghe, *J. Nucl. Med.* **2009**, *50*, 1251 – 1259.
[23] R. Vandenberghe, K. Van Laere, A. Ivanoiu, E. Salmon, C. Bastin, E. Triau, S. Hasselbalch, I. Law, A. Andersen, A. Korner, L. Minthon, G. Garraux, N. Nelissen, G. Bormans, C. Buckley, R. Owenius, L. Thurfjell, G. Farrar, D. J. Brooks, *Ann. Neurol.* **2010**, *68*, 319 – 329.
[24] C. C. Rowe, V. L. Villemagne, *J. Nucl. Med.* **2011**, *52*, 1733 – 1740.
[25] V. L. Villemagne, C. C. Rowe, *Int. Psychogeriatr.* **2011**, *23(Suppl. S2)*, S41 – S49.
[26] A. B. Newberg, N. A. Wintering, K. Plossl, J. Hochold, M. G. Stabin, M. Watson, D. Skovronsky, C. M. Clark, M. P. Kung, H. F. Kung, *J. Nucl. Med.* **2006**, *47*, 748 – 754.
[27] M. P. Kung, C. Hou, Z. P. Zhuang, A. J. Cross, D. L. Maier, H. F. Kung, *Eur. J. Nucl. Med. Mol. Imaging* **2004**, *31*, 1136 – 1145.
[28] M. P. Kung, C. Hou, Z. P. Zhuang, B. Zhang, D. Skovronsky, J. Q. Trojanowski, V. M. Lee, H. F. Kung, *Brain Res.* **2002**, *956*, 202 – 210.
[29] Z. P. Zhuang, M. P. Kung, A. Wilson, C. W. Lee, K. Plossl, C. Hou, D. M. Holtzman, H. F. Kung, *J. Med. Chem.* **2003**, *46*, 237 – 243.
[30] M. Kung, C. Hou, Z. Zhuang, D. Skovronsky, H. F. Kung, *Brain Res.* **2004**, *1025*, 98 – 105.
[31] H. F. Kung, C. W. Lee, Z. P. Zhuang, M. P. Kung, C. Hou, K. Plossl, *J. Am. Chem. Soc.* **2001**, *123*, 12740 – 12741.
[32] R. Chandra, M. P. Kung, H. F. Kung, *Bioorg. Med. Chem. Lett.* **2006**, *16*, 1350 – 1352.
[33] X. Duan, B. Liu, *Sci. China Ser. B* **2008**, *51*, 801 – 807.
[34] E. E. Nesterov, J. Skoch, B. T. Hyman, W. E. Klunk, B. J. Bacskai, T. M. Swager, *Angew. Chem.* **2005**, *117*, 5588 – 5592; *Angew. Chem. Int. Ed.* **2005**, *44*, 5452 – 5456.
[35] J. Qiao, C. Gan, C. Wang, J. Ge, D. Nan, J. Pan, J. Zhou, *J. Nucl. Med. Meeting Abstracts* **2011**, *52*, 82.
[36] D. N. Kevill, E. D. Weiler, N. H. Cromwell, *J. Org. Chem.* **1964**, *29*, 1276 – 1278.
[37] D. L. Yang, X. M. Yu, X. M. Yu, *J. Wuhan Univ. Nat. Sci. Ed.* **1991**, 117 – 119.
[38] W. Qu, M. P. Kung, C. Hou, T. E. Benedum, H. F. Kung, *J. Med. Chem.* **2007**, *50*, 2157 – 2165.
[39] C. Wu, Z. Wang, H. Lei, W. Zhang, Y. Duan, *J. Am. Chem. Soc.* **2007**, *129*, 1225 – 1232.
[40] H. R. Levine, III, *Amyloid* **2005**, *12*, 5 – 14.
[41] R. Nelson, M. R. Sawaya, M. Balbirnie, A. O. Madsen, C. Riekel, R. Grothe, D. Eisenberg, *Nature* **2005**, *435*, 773 – 778.
[42] H. Sugimoto, Y. Yamanishi, Y. Iimura, Y. Kawakami, *Curr. Med. Chem.* **2000**, *7*, 303 – 339.
[43] V. Tomeckova, M. Poskrobova, M. Stefanisinova, P. Perjesi, *Spectrochim. Acta Part A* **2009**, *74*, 1242 – 1246.
[44] Y. Huang, M. Q. Zheng, J. M. Gerdes, *Curr. Top. Med. Chem.* **2010**, *10*, 1499 – 1526.
[45] R. N. Waterhouse, *Mol. Imaging Biol.* **2003**, *5*, 376 – 389.
[46] L. Cai, J. S. Liow, S. S. Zoghbi, J. Cuevas, C. Baetas, J. Hong, H. U. Shetty, N. M. Seneca, A. K. Brown, R. Gladding, S. S. Temme, M. M. Herman, R. B. Innis, V. W. Pike, *J. Med. Chem.* **2008**, *51*, 148 – 158.
[47] X. H. Duan, J. P. Qiao, Y. Yang, M. C. Cui, J. N. Zhou, B. L. Liu, *Bioorg. Med. Chem.* **2010**, *18*, 1337 – 1343.
[48] M. P. Kung, C. Hou, S. Oya, M. Mu, P. D. Acton, H. F. Kung, *Eur. J. Nucl. Med.* **1999**, *26*, 844 – 853.
[49] W. E. Klunk, Y. Wang, G. F. Huang, M. L. Debnath, D. P. Holt, L. Shao, R. L. Hamilton, M. D. Ikonomovic, S. T. DeKosky, C. A. Mathis, *J. Neurosci.* **2003**, *23*, 2086 – 2092.
[50] Y.-C. Cheng, W. H. Prusoff, *Biochem. Pharmacol.* **1973**, *22*, 3099 – 3108.
[51] M. Zheng, D. Yin, J. Qiao, L. Zhang, Y. Wang, *J. Fluorine Chem.* **2008**, *129*, 210 – 216.
[52] N. Okamura, T. Suemoto, H. Shimadzu, M. Suzuki, T. Shiomitsu, H. Akatsu, T. Yamamoto, M. Staufenbiel, K. Yanai, H. Arai, H. Sasaki, Y. Kudo, T. Sawada, *J. Neurosci.* **2004**, *24*, 2535 – 2541.
[53] M. C. Cui, Z. J. Li, R. K. Tang, B. L. Liu, *Eur. J. Nucl. Med.* **2010**, *18*, 2777 – 2784.
[54] H. D. Hill, J. G. Straka, *Anal. Biochem.* **1988**, *170*, 203 – 208.

Received: April 1, 2012
Published online on July 6, 2012

